

Whole-Cell Recordings in Freely Moving Rats

Neurotechnique

Albert K. Lee,^{1,*} Ian D. Manns,² Bert Sakmann,² and Michael Brecht^{1,2,*}

¹Department of Neuroscience

Erasmus MC

Dr. Molewaterplein 50

3015 GE Rotterdam

The Netherlands

²Department of Cell Physiology

Max-Planck Institute for Medical Research

Jahnstrasse 29

69120 Heidelberg

Germany

Summary

Intracellular recording, which allows direct measurement of the membrane potential and currents of individual neurons, requires a very mechanically stable preparation and has thus been limited to *in vitro* and head-immobilized *in vivo* experiments. This restriction constitutes a major obstacle for linking cellular and synaptic physiology with animal behavior. To overcome this limitation we have developed a method for performing whole-cell recordings in freely moving rats. We constructed a miniature head-mountable recording device, with mechanical stabilization achieved by anchoring the recording pipette rigidly in place after the whole-cell configuration is established. We obtain long-duration recordings (mean of ~20 min, maximum 60 min) in freely moving animals that are remarkably insensitive to mechanical disturbances, then reconstruct the anatomy of the recorded cells. This head-anchored whole-cell recording technique will enable a wide range of new studies involving detailed measurement and manipulation of the physiological properties of identified cells during natural behaviors.

Introduction

Understanding complex behaviors in terms of the activity of individual neurons is a central goal of neuroscience. So far, extracellular recording of the action potential (AP) activity of single neurons has been the key technique for revealing cellular correlates of behavior in awake (Evarts, 1968; Georgopoulos et al., 1982) and freely moving (O'Keefe and Dostrovsky, 1971; Taube et al., 1990) animals. However, our knowledge could be considerably extended by intracellular recordings. Such recordings measure not only the suprathreshold AP output of a neuron, but also its subthreshold synaptic inputs and fluctuations in terms of both membrane potential and current, as well as properties such as the spike threshold and input resistance. Furthermore, intracellular recording allows manipulation of the cell's membrane potential through direct current injection

and filling of the cell for subsequent anatomical reconstruction of its location and geometry. Because of the effect of network circuitry, neuromodulators, and behavioral state on single-neuron activity, there is great value to performing these recordings in freely behaving animals. In particular, detailed cellular mechanisms revealed by *in vitro* cellular and molecular studies could be tested for their relevance during natural behaviors.

The major technical problem with obtaining and maintaining intracellular recordings is that the recordings require direct physical contact between recording pipette and neuronal membrane. Thus, compared to extracellular recordings, a much more stable experimental arrangement is necessary. The vast majority of intracellular recordings are currently performed *in vitro*, where the pipette-to-cell connection is not subjected to the transient (behavior-related) and periodic (breathing- and heartbeat-related) movements of the animal and brain that occur *in vivo*. Previous work on intracellular recording *in vivo* has involved preparations in which the animal's head is rigidly fixed relative to a stationary, and usually large, experimental apparatus. In these studies, both types of intracellular recording with glass pipettes have been used: sharp microelectrode recording, which requires penetration of the cell membrane by the pipette tip, and whole-cell recording, which involves attachment of the tip to a small patch of the membrane. Most of these recordings have been performed in anesthetized animals to further minimize disruptive movements. Intracellular recordings in awake, head-fixed animals have been obtained with sharp microelectrodes in fish (Aksay et al., 2001), rats (Fee, 2000), rabbits (Swadlow et al., 1998), cats (Baranyi et al., 1993a, 1993b; Steriade et al., 2001), and primates (Yokota et al., 1970; Matsumura et al., 1996; Chen and Fetz, 2005), and with whole-cell pipettes in fish (Aksay et al., 2001), bats (Covey et al., 1996), and rats (Margrie et al., 2002; Brecht et al., 2004). Recently, an active compensation system was developed in order to improve the mechanical stability of intracellular recordings (Fee, 2000). By moving the pipette in synchrony with measured and predicted brain surface movements, it was possible to obtain sharp microelectrode recordings in head-fixed rats running on a treadmill (Fee, 2000). In an alternative approach to using pipettes, a miniature two-photon imaging device capable of measuring intracellular $[Ca^{2+}]$ transients was developed and mounted on the heads of rats (Helmchen et al., 2001), though the stabilization problem was not solved.

Here we describe a technique we have developed for intracellular recording in non-head-fixed, freely moving animals. We have chosen to adapt whole-cell recording for this purpose because such recordings display favorable properties with respect to mechanical stability (Margrie et al., 2002). We will describe the miniaturization of the recording device, the stabilization method, and the performance of the technique in freely moving rats.

*Correspondence: a.lee@erasmusmc.nl (A.K.L.); m.brecht@erasmusmc.nl (M.B.)

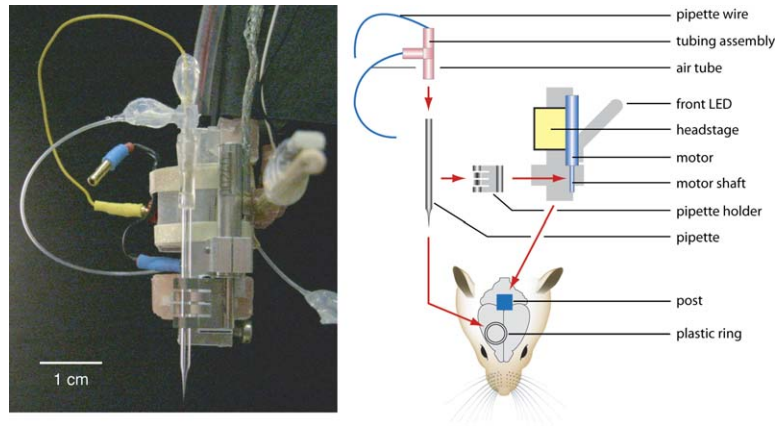


Figure 1. Miniature Head-Mountable Whole-Cell Recording Device

(Left) Photograph of front view of the device. (Right, top) Corresponding diagram that identifies the device components and shows how they are connected to each other. The device contains a piezoelectric motor that advances the pipette into the brain in micron-sized steps necessary for performing blind, *in vivo* whole-cell recording, a patch-clamp amplifier headstage that measures the membrane potential and currents and can inject current, and LEDs that are used to track the animal's head position and direction. The recording pipette is connected to the motor shaft via the pipette holder and to the pipette recording wire and air pressure tube via the tubing assembly piece. The total weight of the device is 20 g. (Right, bottom) View of the animal's head from above. The bottom of the device mounts onto a post attached to the head. The pipette is positioned above a plastic ring that surrounds the brain exposure.

Results

Miniaturization of the Whole-Cell Recording Device

The equipment for recordings had to be miniaturized in size and weight so that it could be carried by a small (50–100 g), freely moving rat. Using larger rats was not a preferable option due to the lower probability of obtaining low access resistance whole-cell recordings from older animals (Margrie et al., 2002).

Headstage

To obtain low interference noise recordings, it is essential to amplify signals close to the signal source. While very small headstages for extracellularly recorded signals have long been available, no small headstages for whole-cell recording were available at the beginning of our study. We therefore asked ABIMEK (Göttingen, Germany) to design one. The result, the PA-50MM, is a resistor feedback headstage with dimensions of 14 × 14 × 12 mm (Figure 1) that connects to the amplifier (WPC-100) via a light, flexible, 3 m long cable. Miniaturization was achieved by unifying all the electronic components on a single sealed hybrid circuit. Also, while the full-size headstage from ABIMEK can be switched between a 50 and a 0.5 gigaohm (GΩ) resistive feedback element (for performing single-channel and whole-cell recordings, respectively), the PA-50MM has only a single 0.5 GΩ resistor, i.e., it is designed exclusively for whole-cell recordings. The PA-50MM has all the features of a standard whole-cell recording headstage, including current injection and both voltage- and current-clamp modes. We first attached this device to a standard micromanipulator and tested it in anesthetized animals. High-quality recordings, indistinguishable from those obtained with standard headstages, were obtained as described previously (Margrie et al., 2002).

Micromanipulator

The pipette must be moved toward the cell with micron resolution to obtain whole-cell recordings. We screened a variety of small motors and early on chose piezoelectric stepping motors. These motors step (advance) with submicron resolution and have several favorable properties for our application: (1) small size, (2) robustness,

(3) long range, (4) considerable force when stepping, (5) minimal drift, and (6) a large static holding force (i.e., they can maintain their position against applied forces), even when the power is turned off. We tested several different piezoelectric motors and in all cases obtained high-quality, blind (i.e., without visual guidance) whole-cell recordings in anesthetized animals. However, all of the motors showed considerable trial-to-trial variability (up to a factor of 2) of the depth to which a pipette is advanced by each step. This is a serious limitation, so during each recording attempt we visually monitored the distance advanced over 100–200 steps, estimated the average step size, then adjusted the controls to give the desired value (2–4 μm). We currently use the smallest of the motors, the NM2104 (21 mm long, 4 mm diameter, 7 mm range; Figure 1), made by Kleindiek Nanotechnik (Reutlingen, Germany).

Pipette Holder

Minimizing the size and weight of the pipette-carrying construct was of critical importance, both because a smaller load improved motor performance and because this reduces the forces that act on the recording pipette. Our current design was developed by Kleindiek Nanotechnik (following an initial suggestion from U. Egert). It consists of a small metal holder that connects the pipette to the motor shaft and a separate tubing assembly for the recording wire and air pressure (Figure 1). Note that both the wire and pressure tubing are very flexible and thus exert only minimal forces on the recording pipette.

Head-Mountable Assembly

We constructed a miniature head-mountable device (Figure 1) containing all the components described above along with light-emitting diodes (LEDs) for tracking the animal's head position and direction. The LEDs are placed at each end of a thin bar that extends 4 cm in front of and 4 cm in back of the device. The overall dimensions of the device are 37 × 22 × 15 mm, excluding the LED extension. The overall weight is 20 g including the LEDs but excluding the cabling. With this device attached to a standard stereotaxic surgical apparatus (i.e., not head-mounted), we successfully obtained

whole-cell recordings from anesthetized rats ($n = 25$ neurons: 12 from barrel cortex, eight from hippocampus [hc], five from hindlimb motor cortex). The device is (reversibly) mounted on the animal's head by screwing it to a post attached to the skull (Figure 1). As with extracellular recordings in freely moving rodents, a pulley and counterweight system offsets the weight of the device and its cabling to help the animal carry it.

Stabilization of Intracellular Recordings

Three major factors allowed us to achieve the stabilization necessary for obtaining intracellular recordings in freely moving animals.

First, the $G\Omega$ seal formed between the pipette tip glass and the cell membrane is stable (Hamill et al., 1981). It reduces the effect of micron-range movements, as evidenced by the sudden elimination of the heartbeat artifact upon forming the seal in vivo (Margrie et al., 2002). It is well known that once a $G\Omega$ seal has been established, the pipette can be moved many microns away from the cell without compromising the attachment between membrane and pipette (Hamill et al., 1981).

Second, by making the recording apparatus small and light and mounting it directly on the head (i.e., fixing it to the skull, close to the recording site), the stability of our recordings was improved over standard in vivo whole-cell recordings. In anesthetized preparations, we could gently shake the stereotaxic apparatus holding the animal without losing the recording, perhaps due to smaller relative movements and forces. However, these measures are not sufficient for freely moving recordings, as seen by the loss of the recording upon removing the animal from the stereotaxic apparatus.

The third, and key, factor is the rigid anchoring of the pipette relative to the head. Prior to this anchoring step the pipette can move, both because the stepping motor has a cylindrical shaft around which the pipette holder can rotate (Figure 1) and because the lightweight components of the head-mounted assembly have an intrinsically limited rigidity. Before a whole-cell recording is obtained, the recording well is filled with a layer (~1–2 mm thick) of agar that surrounds the pipette and covers the brain (Figure 2). Once a whole-cell recording is obtained, a thin (~0.5–1 mm) layer ("pipette anchoring layer") of dental acrylic (Paladur, Heraeus Kulzer, Hanau, Germany) is carefully applied around the pipette, connecting it to the previously hardened dental acrylic ("acrylic base") that is fixed to the skull via bone screws (Figure 2). This layer hardens in ~5 min, fixing the pipette in place. The agar simultaneously protects the brain surface from the acrylic and acts to hold the tissue in place. The stability provided by the agar-acrylic anchoring was tested on whole-cell recordings in anesthetized animals ($n = 4$ neurons). We applied a series of abrupt mechanical disturbances to the stereotaxic apparatus (which cause immediate recording loss in standard preparations), and in all cases the recording was not lost. In one case we removed the animal from the stereotaxic apparatus and moved the animal around in a variety of postures, again without losing the recording. These results suggested that the stabilization achieved would be sufficient for freely moving recordings.

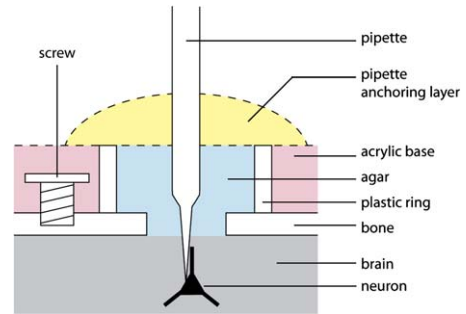


Figure 2. Head-Anchored Pipette Stabilization Method

Dental acrylic (pink) secures a plastic ring and a head post (not shown) to the skull via screws. The plastic ring surrounds the brain exposure. The recording device (not shown) is mounted onto the head post (Figure 1). A pipette is then lowered into the brain, agar is added into the ring, and the pipette is advanced in steps to establish a $G\Omega$ seal on a neuron. After a whole-cell recording has been established, a layer of adhesive material (yellow) is carefully applied around the pipette to anchor it rigidly to the dental acrylic base and, thus, to the head.

Head-Anchored Whole-Cell Recordings from Freely Moving Rats

Recordings were made from neurons in the right hindlimb primary motor cortex (ctx) and the CA1 subregion of the right dorsal hc of 22- to 28-day-old male Wistar rats. The whole-cell recording configuration was first established in an animal anesthetized with a rapidly antagonizable anesthetic, and then the pipette was anchored in place. The rat was then injected with the antagonist to the anesthetic and gently moved from the surgical apparatus to the behavioral arena where it would wake up 1–3 min later.

Motor Cortex

Data recorded from a neuron in the primary hindlimb motor cortex are shown in Figure 3. The cell was filled with biocytin during the recording and later reconstructed. It was a layer 3 pyramidal neuron with a thick-tufted dendritic arbor and an extensive local axonal arbor, both restricted to hindlimb motor cortex, and a callosal projection (Figure 3A). The recording lasted for 1 hr after the rat woke up. A 5 min period during which the rat ran all around the arena is shown in Figures 3B and 3C. The current-clamp trace shows a stable baseline membrane potential and large-amplitude (>90 mV) APs that overshoot 0 mV (Figure 3C, top, and Figure 3D). The animal's movements were not associated with any obvious artifacts, as illustrated by a close-up of the membrane potential trace while the rat ran at high speed (Figure 3E). The recording declined in quality after the first 10 min, as indicated by an increase in series resistance and a small depolarization. During the recording we applied brief puffs of air to various parts of the skin. This procedure required several minutes and involved a variety of mechanical manipulations such as gently holding the animal's paws. Consistent with the topographic position of the neuron (Figure 3A), sensory responses were evoked upon contralateral hindpaw stimulation, with a subthreshold postsynaptic potential of approximately 10 mV (data not shown). Voltage-clamp recordings from motor cortical neurons were also obtained (data not shown). From these experiments and additional

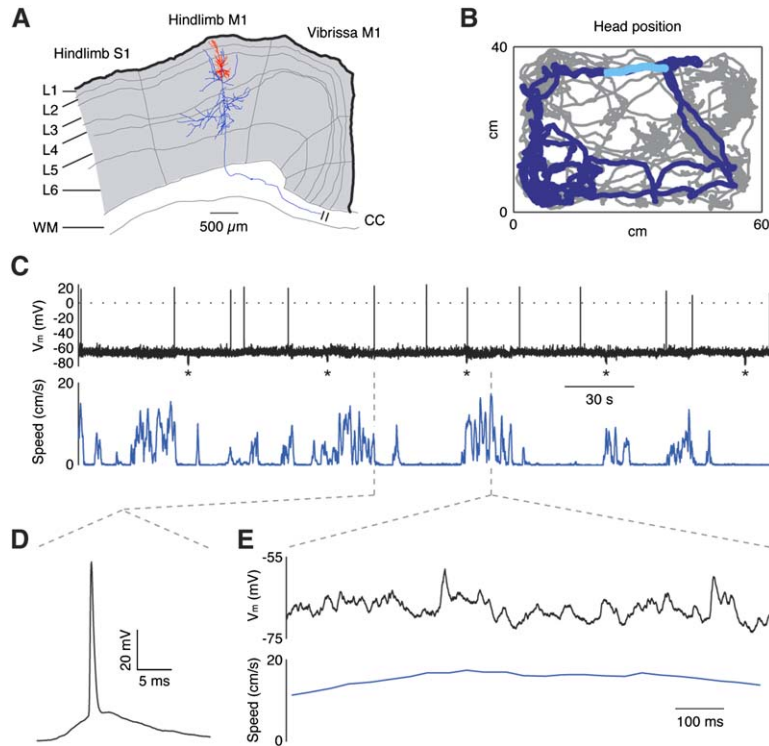


Figure 3. Whole-Cell Recording of a Hindlimb Motor Cortex Neuron in a Freely Moving Rat (A) Reconstruction of the axonal (blue) and dendritic (red) arbors of this layer 3 pyramidal neuron.

(B) Top view of the behavioral arena, showing the trajectory of the rat's head position for the entire 1 hr duration of this recording (all colors together).

(C) Membrane potential (black, top) over a 5 min period during which the rat moved freely around the arena (dark blue line in [B], distance traveled = 545 cm), and the corresponding speed of head movement (blue, bottom). Asterisks below voltage trace mark five responses to 500 ms 0.3 nA hyperpolarizing pulses used to probe the series and input resistance, here 19.3 ± 1.5 and 26.0 ± 6.4 M Ω (mean \pm standard deviation), respectively.

(D) An example action potential (AP).

(E) Subthreshold membrane potential trace (black, top) over a 1 s period during which the rat ran at high speed (blue, bottom) along the light blue segment shown in (B).

M1 = primary motor cortex, S1 = primary somatosensory cortex, L1–L6 = cortical layers 1 through 6, WM = white matter, CC = corpus callosum.

ones performed in anesthetized animals, it appears that the voltage-clamp performance of the device is similar in quality to what we have obtained previously (Brecht et al., 2005).

Hippocampus

Whole-cell recordings in the hippocampus of freely moving rodents are of considerable interest since the rodent hippocampus is a model system for studying synaptic plasticity and spatial memory formation (Martin et al., 2000). However, recordings of hippocampal principal neurons pose experimental difficulties because a thin layer of cells relatively deep in the brain needs to be targeted. Preliminary experiments in anesthetized animals showed we could successfully target hippocampal neurons (as verified histologically). We were also able to record a hippocampal cell in a freely moving animal. This neuron too was filled and reconstructed, indicating that it was a pyramidal cell from area CA1 (Figure 4A). The recording lasted for 21 min after the rat woke up. Again, while the rat moved around the arena (Figure 4B), the baseline membrane potential was stable with large-amplitude, overshooting APs (Figure 4C, top, and Figure 4E). In this case, the rat was not very active, though it did move its head around and run for a few brief spurts. During one of the head turns, the membrane potential trace displayed oscillatory activity in the theta (6–12 Hz) range (Figure 4D), possibly an intracellular correlate of hippocampal EEG theta activity (Vanderwolf, 1969).

Mechanical Artifacts

The recording duration and its maintenance during the animal- and experimenter- induced movements (including the removal of the rat from the stereotaxic apparatus and the transfer to the arena) demonstrate the stability of the method. Putative mechanical artifacts were

evoked when the recording device bumped into the wall of the arena (Figure 5A). Such bumps sometimes but not always resulted in brief transients, and afterwards the membrane potential would return to its previous level. The example in Figure 5A is from the same cell shown in Figure 3. This bump occurred 30 s after the start of the trace shown in Figure 3C; thus, high-quality recordings can continue after such mechanical disturbances. As an additional, extreme test of mechanical stability, we performed a “crash test.” The rat was placed on a small, moderately unstable, 8 cm high platform from which it jumped to the arena floor. This resulted in a brief, large transient, but afterwards the membrane potential returned to its original level (Figure 5B). The average membrane potential during the 5 min period centered on the crash shows only a slight 2 mV depolarization (Figure 5B).

Success Rate

We defined a recording as successful if, after the animal woke up, both (1) the membrane potential was ≤ -55 mV and (2) the series resistance was <100 M Ω . In a first set of head-mounted experiments, whole-cell recordings were obtained and the pipette anchored in place using dental acrylic for a total of 27 neurons (ctx = 16, hc = 11). Four recordings satisfied our criteria for success, while 23 recordings were lost (21 in which the membrane potential depolarized to >-55 mV before the animal was awoken. Only one of the losses occurred while initially applying the dental acrylic, and only two while removing the animal from the surgical apparatus and transferring it into the arena. Many of the other 20 losses occurred approximately 5 min after the acrylic was first applied, perhaps due to shrinkage of the acrylic during hardening and a resulting movement of the pipette. In fact, three of the four successes also displayed a period of depolarization

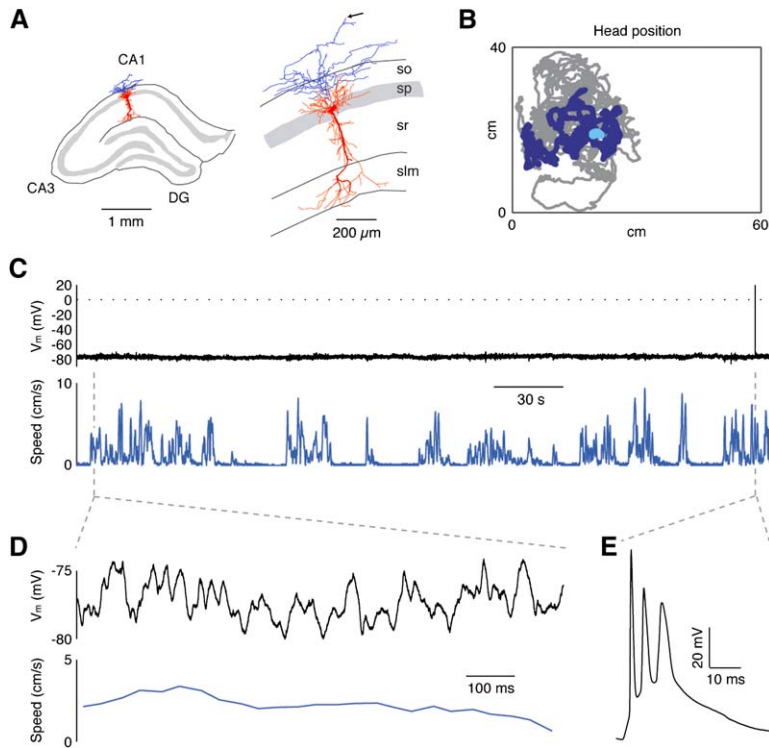


Figure 4. Whole-Cell Recording of a Hippocampal Neuron in a Freely Moving Rat

(A) Reconstruction of the axonal (blue) and dendritic (red) arbors of this CA1 pyramidal neuron at lower (left) and higher (right) magnification. Arrow indicates the main axonal branch that extended for 2 mm perpendicular to the image plane.

(B) Top view of the behavioral arena, showing the trajectory of the rat's head position for the entire 21 min duration of this recording (all colors together).

(C) Membrane potential (black, top) over a 5 min period during which the rat moved freely around the arena (dark blue line in [B], distance traveled = 293 cm), and the corresponding speed of head movement (blue, bottom).

(D) Subthreshold membrane potential trace (black, top) and speed of head movement (blue, bottom) during a head turn (light blue segment shown in [B]).

(E) An AP triplet.

DG = dentate gyrus, so = stratum oriens, sp = stratum pyramidale, sr = stratum radiatum, slm = stratum lacunosum-moleculare.

around the same time before recovering. Thus, many recordings are lost during the pipette anchoring process. However, once anchoring is achieved, the recordings are stable and resistant to mechanical disturbances, many of which are very severe. The data in Figures 3 to 5 all come from experiments using dental acrylic as the anchoring material. In an attempt to improve the success rate, we tested two other materials for the anchoring layer, both chosen because they shrink much less than dental acrylic during hardening: versyo.com (Heraeus Kulzer), a visible light-cured adhesive, and Dymax 3021 (Dymax, Torrington, CT), a UV-cured adhesive with almost no shrinkage. The success rate was 1/9 (ctx = 9) using versyo.com (with most recordings lost during curing) and 2/7 (ctx = 7) using Dymax 3021 (with five recordings exhibiting no depolarization during curing, though three of those were lost while removing the animal from the surgical apparatus, leaving two successes). Thus, Dymax 3021 displays two promising properties compared to dental acrylic: a higher success rate and fewer losses during hardening.

Table 1 gives an overview of the seven successful recordings obtained in freely moving animals (ctx = 6, hc = 1). The mean duration of the recordings was 18.7 min, with a maximum of 60.3 min. The duration represents only the period after the animal woke up in which both the average membrane potential remained ≤ -55 mV and the series resistance remained <100 M Ω , and does not include the 10–15 min from the establishment of the whole-cell configuration to the moment of waking. Six recordings ended due to depolarization >-55 mV, and one because the series resistance increased to >100 M Ω . Animals covered substantial distances during the recordings (mean = 1336 cm, i.e., 71 cm/min), as measured from the tracked head position. In order to

assess if our experimental animals show comparable motor activity to animals that had not been drugged, we tracked movements in rats that did not undergo the anesthesia-antagonist-wake-up process but were carrying the same recording device (and, like the experimental animals, were not previously trained to carry it). We found that these animals traveled similar distances (mean = 85 cm/min). Cells generally had low AP firing rates (mean = 0.36 Hz). Series and input resistance values were generally stable across multiple measurements during the recordings (the coefficient of variation of these values during each recording averaged across recordings equals 0.17 and 0.22, for series and input resistance, respectively). Four neurons could be recovered (out of six attempted recoveries) for morphological reconstructions. Neurons were well-filled (Figures 3A and 4A) and none were visibly mechanically damaged by the recording.

Discussion

We have described a miniature recording device and pipette stabilization technique that allows one to obtain high-quality, long-lasting whole-cell recordings in freely moving animals. To the best of our knowledge, these are the first intracellular recordings from freely moving animals in the literature, as well as the first intra- or extracellularly recorded neurons from freely moving animals to be anatomically reconstructed.

Several observations suggest that the neurons we recorded were in excellent physiological condition: (1) average membrane potential values compare to what has been found in other awake animal recordings, (2) membrane potentials were stable over time and fluctuations were in the range of what has been described under

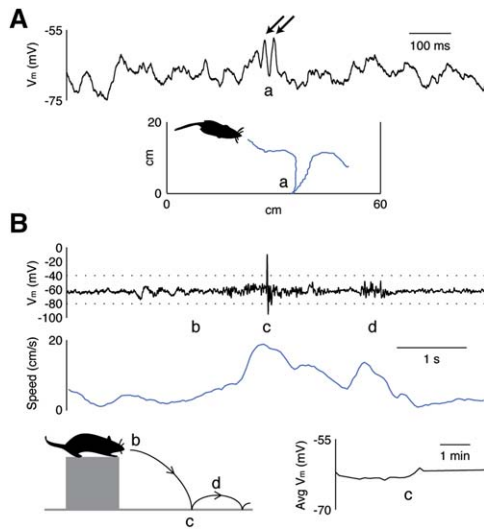


Figure 5. Recordings Are Stable against Mechanical Disturbances
(A) Membrane potential trace (black, top) around the time (a) that the rat bumps the recording device into the arena wall (front LED trajectory: blue, bottom). Note the brief transient (two arrows) after which the membrane potential continues as before.
(B) Membrane potential trace (black, top) during an extreme test of the head-anchored recording's stability. Rat sits on platform 8 cm above the arena floor, starts to jump off (b), crashes onto the arena floor (c), then takes another hop (d), with corresponding head speed (with respect to the plane parallel to the arena floor) (blue, middle). This results in a large transient (no AP occurs) at (c), but afterwards the membrane potential returns to its previous level. (Bottom, right) Average membrane potential (averaged over 10 s) for the 5 min around (c).

awake conditions, (3) input resistances compare to values from whole-cell cortical recordings in anesthetized and awake rats (Margrie et al., 2002; Brecht and Sakmann, 2002; Brecht et al., 2003; Manns et al., 2004), (4) the long duration of the recordings, (5) histological recovery of many of the recorded neurons without signs of leakage or mechanical damage, and (6) the low AP firing rates, which are characteristic of whole-cell cortical recordings in anesthetized and awake animals (Margrie et al., 2002). The latter result suggests that low cortical firing rates (Olshausen and Field, 2004; Brecht et al., 2005) are a general phenomenon that extends to freely behaving animals, and the low hippocampal firing rate is consistent with extracellular recordings in freely mov-

ing rodents showing that over half of CA1 neurons are “silent” (i.e., fire very few APs) in any given environment (Muller, 1996). In addition, series resistances were stable, compare to values from anesthetized and awake animal whole-cell recordings (Margrie et al., 2002), and were in several cases relatively low (which is a requirement for voltage-clamp experiments).

Long-duration intracellular recordings in awake, head-fixed animals have been obtained previously (Yokota et al., 1970; Baranyi et al., 1993a, 1993b; Covey et al., 1996; Swadlow et al., 1998; Fee, 2000; Aksay et al., 2001; Steriade et al., 2001; Margrie et al., 2002; Chen and Fetz, 2005). In awake, head-fixed rats, whole-cell recordings can be quite stable (Margrie et al., 2002) as long as the animals sit still and do not try to move. Recording duration and quality drop when overt behaviors such as whisking movements are evoked by applying sensory stimuli. Under such conditions the average recording duration is only ~7 min and the fraction of neurons that can be recovered for histological reconstruction is low (M.B. and B.S., unpublished data). An unexpected result of our study is the endurance of our recordings even under conditions of severe mechanical disturbance such as the crash illustrated in Figure 5B. Our sample is small, but it appears that the average duration of our recordings is in the same range as what is obtained with whole-cell cortical recordings in anesthetized preparations (Pei et al., 1991; Ferster and Jagadeesh, 1992; Moore and Nelson, 1998; Zhu and Connors, 1999; Margrie et al., 2002). Thus, the stability gained by head-anchoring the pipette appears to at least compensate for the added mechanical disturbance of the freely moving preparation. In addition, the tight sealing of the brain exposure by the agar-anchor-material cover, which limits brain pulsations and movements, is likely to contribute to stability. Head-anchoring of the pipette would also likely improve stability in awake, head-fixed experiments.

At this stage it is still considerably more difficult to obtain a head-anchored whole-cell recording in a freely moving animal than a standard in vivo whole-cell recording in an animal that remains head-fixed and anesthetized. In particular, the loss of recordings during the pipette anchoring process significantly diminishes the success rate. Dymax 3021 greatly improves the number of recordings that survive the hardening step and also improves the number of successful recordings compared to dental acrylic. While the resulting duration appears to be lower in this limited sample (possibly due

Table 1. Summary of the Seven Whole-Cell Recordings from Freely Moving Rats

Brain area	Anchoring method	Recording duration (min)	Distance traveled (cm)	Mean membrane potential (mV)	Mean AP firing rate (Hz)	Mean input resistance (MΩ)	Mean series resistance (MΩ)
hc	dental acrylic	21.3	1641	-73.7	0.045	50	30
ctx	dental acrylic	22.0	1616	-64.1	0.028	15*	15*
ctx	dental acrylic	12.0	818	-59.0	0.008	26	60
ctx	dental acrylic	60.3	3385	-61.1	0.282	18	40
ctx	versyo.com	0.5	110	-66.6	0.226	N.A.	80
ctx	Dymax 3021	7.3	1039	-71.4	0.156	13	80
ctx	Dymax 3021	7.8	742	-61.4	1.797	34	74

Neurons were located in hindlimb primary motor cortex (ctx) or the CA1 subregion of dorsal hippocampus (hc). The recording duration, distance traveled, mean membrane potential, mean AP firing rate, mean input resistance, and mean series resistance refer to the period after the animal woke up during which the average membrane potential (averaged every 10 s) was ≤ -55 mV and the series resistance was <100 MΩ. The exceptions are the values marked (*), which were measured only under anesthesia.

to lower hardness), using a combination of Dymax 3021 followed by dental acrylic could address such a problem. Most importantly, however, the successful dental acrylic-anchored recordings demonstrate that passive, rigid stabilization is sufficient for long, high-quality recordings.

A disadvantage of our current arrangement is that after anchoring the pipette in place, a quick removal and replacement is not possible. Restricting the anchoring material to an exchangeable ring would fix this problem. Another limitation is that we first obtained the recordings under anesthesia and only then woke up the animal. This was to simplify our experimental procedures so that we could focus on the stabilization method. However, we should be able to obtain and anchor recordings in awake, head-fixed animals trained to remain relatively still (Margrie et al., 2002), thus eliminating any effects of the anesthetic and antagonist on the physiology. Lastly, we did not miniaturize the recording device beyond what was necessary for the size of rats we used. Further miniaturization is ongoing, and thus the method should soon be adaptable to mice.

Head-anchored whole-cell recording in freely moving animals will enable a new range of studies of neurons whose activity is only or best observable during natural behaviors, such as those with spatial, running, turning, mating, exploring, or other motor correlates. Such experiments will be instrumental for integrating results from *in vitro* culture and slice preparations with results from *in vivo* extracellular recordings and behavioral studies. For instance, since subthreshold activity reflects the synaptic inputs to a cell, the synaptic plasticity correlates of behavioral learning and memory can be measured. Furthermore, whole-cell recording allows one to stimulate or suppress AP firing in the recorded cell through direct current injection (while leaving all other cells alone), therefore allowing one to test how various plasticity induction rules that do (Markram et al., 1997; Bi and Poo, 1998) or do not (Golding et al., 2002) depend on somatic spiking of the postsynaptic cell might function during behavior. Thus, head-anchored whole-cell recordings could help elucidate the link between cellular phenomena such as long-term potentiation/depression and systems properties such as spatial memory (Martin et al., 2000). In addition, anatomical reconstruction of the recorded cells will reveal new relationships between neuron type, connectivity, and function.

Experimental Procedures

Surgery

All experimental procedures were carried out according to Dutch guidelines on animal welfare under the supervision of a local (DEC) ethics committee. Early experiments were performed with P22-P31 male Wistar and Sprague-Dawley rats under urethane (1.4 g/kg) anesthesia. Head-mounted freely moving experiments were performed with P22-P28 male Wistar rats (50–100 g). The animal was anesthetized with an intraperitoneal dose of a mixture of Dormitor (Medetomidine, Roche, 300 μ g/kg), Dormicum (Midazolam, Roche, 8 mg/kg) and Fentanyl (Janssen-Cilag, 10 μ g/kg), then head-fixed (using ear bars and a tooth bar) into a standard stereotaxic surgical apparatus. Additional doses (each 1/4 of the initial dose) were administered approximately every 40 min. Breathing was monitored and the temperature maintained at $37^{\circ}\text{C} \pm 0.5^{\circ}\text{C}$. Five or six gold-plated screws were attached to the exposed skull surface. A small hole

(~ 2 mm diameter) was made in the bone above the desired brain coordinates (hindlimb motor cortex: 1 mm posterior of bregma, 2.5 mm lateral of midline; hippocampus: 3.5 mm posterior of bregma, 2.5 mm lateral of midline). A plastic ring (1–2 mm high, 4–6 mm diameter) and reference wire were placed around the hole and then cemented to the screws using dental acrylic (acrylic base, Figure 2). The device and its detachable post were locked together and positioned over the head so that the pipettes would be centered in the hole; the post was then cemented to the head with additional dental acrylic.

Electrophysiology and Stabilization

Before attempting a recording, the device was first detached from the post and moved away from the head, a new pipette was attached to the device, and the assembly was reattached to the post. The electrode was then advanced into the brain for recording. Blind, *in vivo* whole-cell recordings were obtained using previously described procedures (Margrie et al., 2002). Pipettes (4–6 M Ω , overall length ~ 30 mm, pulled from borosilicate glass with an outer diameter of 1.5 mm) were filled with an intracellular solution containing (in mM) either K-gluconate 135, HEPES 10, Na₂-phosphocreatine 10, KCl 4, MgATP 4, and Na₃GTP 0.3 (pH adjusted to 7.2), or K-gluconate 120, sucrose 17.5, KOH 10, HEPES 10, KCl 9, NaCl 4, Na₂ATP 4, MgCl₂ 3.48, and Na₃GTP 0.4 (pH adjusted to 7.25), as well as biocytin (0.3%–1%). After the pipette was lowered into the brain, but before advancing the pipette in steps (2–4 μ m) to search for a cell, the plastic ring was filled (using a syringe) with a solution of agarose powder (2%) mixed in Ringer's solution containing (in mM) NaCl 135, KCl 5.4, HEPES 5, CaCl₂ 1.8, and MgCl₂ 1 (pH adjusted to 7.2). After a whole-cell recording was obtained, a pipette anchoring layer of dental acrylic, versyo.com, or Dymax 3021 was carefully applied (using a syringe) over the agar and around the pipette in order to connect the pipette to the acrylic base (Figure 2). Dental acrylic hardened in air in ~ 5 min. Versyo.com was hardened by shining 90–120 s of blue light from a handheld curing unit (Translux Power Blue, Heraeus Kulzer), and Dymax 3021 was hardened by shining 10 0.2 s pulses of UV light (with successive pulses separated by 10 s) from an industrial curing unit (BlueWave 50, Dymax). After hardening, the anesthesia was antagonized with a subcutaneous dose of a mixture of Atipamezole, Roche, 1.33 mg/kg, Anexate (Flumazenil, Roche, 800 μ g/kg) and Nalcant (Naloxone, Bristol-Myers Squibb, 240 μ g/kg) (with the dose adjusted to match the total amount of anesthetic administered). Then the animal was removed from the stereotaxic apparatus and moved to the behavioral arena. The animal generally woke up within 1–3 min. Neural data was low-pass filtered at 3 kHz by the patch-clamp amplifier, then sampled at 10 or 20 kHz by a LIH 1600 acquisition interface (HEKA Elektronik, Lambrecht, Germany) under the control of Patchmaster software (HEKA Elektronik). Recordings were corrected for the junction potential.

Behavior

The behavioral arena was a 60 \times 40 cm rectangle with a 20 cm high wall placed inside a large Faraday cage. To minimize the effect of the size and weight of the recording device and cabling on the animal's behavior, a pulley and counterweight system was constructed. Before surgery, the counterweights were adjusted so that the device and cabling alone (i.e., when not attached to an animal's head) would hang above the arena floor at approximately the height of a rat's head. Head position and direction were sampled at 25 Hz by a Cheetah Video Tracker system (Neuralynx, Tucson, AZ) that tracked the LEDs on the animal's head. This data was time-aligned to the neural data through synchronizing pulses sent out by the LIH 1600 and received by a Cheetah data acquisition system (Neuralynx) running the tracker. A video mixer (Edirol V-4, Roland, Hamamatsu, Japan) was used to create and record a split-screen image of the online HEKA oscilloscope displaying the membrane potential or current and the corresponding animal behavior recorded by either a ceiling-mounted or handheld video camera. This video record was used for a coarse analysis of the data. A combination of the video record and position data was used to evaluate behavior, including bumps into the wall and crash tests.

Histology

At the end of recording, the animal was injected with an overdose of urethane or ketamine, the pipette was pulled out from the brain and

anchoring material, and the animal was perfused transcardially with 0.1 M phosphate-buffered saline followed by a 4% paraformaldehyde solution. The brain was removed, stored overnight in a 10% sucrose solution, embedded in gelatin, frozen, and sectioned coronally into slices 80–100 μm thick. Slices were processed with the avidin-biotin-peroxidase method (Horikawa and Armstrong, 1988) to visualize biocytin-filled cells and Nissl-counterstained (Paxinos and Watson, 1998). Cells were reconstructed using NeuroLucida software (MicroBrightfield, Williston, VT).

Analysis

Analysis was performed using custom-made programs written in Matlab (The MathWorks, Natick, MA). The duration of a freely moving recording was calculated as the amount of time after the rat woke up in which the spontaneous (i.e., without current injection) membrane potential averaged every 10 s was ≤ -55 mV and the series resistance was <100 M Ω . The distance traveled (calculated from the head position sampled every 1 s), mean membrane potential, mean AP firing rate, mean input resistance, and mean series resistance apply to this period. Head speed was calculated from the position data using a 0.5 s smoothing window.

Acknowledgments

We are grateful for the technical contributions of E. Zech and R. Schaefer at ABIMEK; S. Kleindiek and K. Schock at Kleindiek Nanotechnik; A. Brouwer and J. Bos at the Erasmus MC Department of Experimental Medical Instrumentation; R. Rödel, P. Mayer, K. Schmidt, and M. Kaiser at the Max-Planck Institute for Medical Research in Heidelberg; and J. van der Burg, E. Haasdijk, E. Goedknecht, E. Dalm, F. Anjum, and the laboratories of C. Hansel and J.G. Borst at the Erasmus MC Department of Neuroscience. We would also like to thank J.G. Borst, C. Hansel, L. Herfst, A. Houweling, and B. Voigt for valuable discussions and comments on the manuscript. This work was supported by the Max-Planck-Society, Erasmus MC, VIDJ (NWO) and HFSP grants to M.B., and an EMBO Long-Term Fellowship to A.K.L.

Received: January 12, 2006

Revised: June 2, 2006

Accepted: July 3, 2006

Published: August 16, 2006

References

Aksay, E., Gamkrelidze, G., Seung, H.S., Baker, R., and Tank, D.W. (2001). In vivo intracellular recording and perturbation of persistent activity in a neural integrator. *Nat. Neurosci.* 4, 184–193.

Baranyi, A., Szente, M.B., and Woody, C.D. (1993a). Electrophysiological characterization of different types of neurons recorded in vivo in the motor cortex of the cat. I. Patterns of firing activity and synaptic responses. *J. Neurophysiol.* 69, 1850–1864.

Baranyi, A., Szente, M.B., and Woody, C.D. (1993b). Electrophysiological characterization of different types of neurons recorded in vivo in the motor cortex of the cat. II. Membrane parameters, action potentials, current-induced voltage responses and electrotonic structures. *J. Neurophysiol.* 69, 1865–1879.

Bi, G.Q., and Poo, M.M. (1998). Synaptic modifications in cultured hippocampal neurons: dependence on spike timing, synaptic strength, and postsynaptic cell type. *J. Neurosci.* 18, 10464–10472.

Brecht, M., and Sakmann, B. (2002). Dynamic representation of whisker deflection by synaptic potentials in spiny stellate and pyramidal cells in the barrels and septa of layer 4 rat somatosensory cortex. *J. Physiol.* 543, 49–70.

Brecht, M., Roth, A., and Sakmann, B. (2003). Dynamic receptive fields of reconstructed pyramidal cells in layers 3 and 2 of rat somatosensory barrel cortex. *J. Physiol.* 553, 243–265.

Brecht, M., Schneider, M., Sakmann, B., and Margrie, T.W. (2004). Whisker movements evoked by stimulation of single pyramidal cells in rat motor cortex. *Nature* 427, 704–710.

Brecht, M., Schneider, M., and Manns, I.D. (2005). Silent Neurons in Sensorimotor Cortices: Implications for Cortical Plasticity. In *Neural*

Plasticity in Adult Somatic Sensory-Motor Systems, F. Ebner, ed. (Boca Raton, FL: CRC Press), pp. 1–19.

Chen, D., and Fetz, E.E. (2005). Characteristic membrane potential trajectories in primate sensorimotor cortex neurons recorded in vivo. *J. Neurophysiol.* 94, 2713–2725.

Covey, E., Kauer, J.A., and Casseday, J.H. (1996). Whole-cell patch-clamp recording reveals subthreshold sound-evoked postsynaptic currents in the inferior colliculus of awake bats. *J. Neurosci.* 16, 3009–3018.

Evarts, E.V. (1968). Relation of pyramidal tract activity to force exerted during voluntary movement. *J. Neurophysiol.* 31, 14–27.

Fee, M.S. (2000). Active stabilization of electrodes for intracellular recording in awake behaving animals. *Neuron* 27, 461–468.

Ferster, D., and Jagadeesh, B. (1992). EPSP-IPSP interactions in cat visual cortex studied with in vivo whole-cell patch recording. *J. Neurosci.* 12, 1262–1274.

Georgopoulos, A.P., Kalaska, J.F., Caminiti, R., and Massey, J.T. (1982). On the relations between the direction of two-dimensional arm movements and cell discharge in primate motor cortex. *J. Neurosci.* 2, 1527–1537.

Golding, N.L., Staff, N.P., and Spruston, N. (2002). Dendritic spikes as a mechanism for cooperative long-term potentiation. *Nature* 418, 326–331.

Hamill, O.P., Marty, A., Neher, E., Sakmann, B., and Sigworth, F.J. (1981). Improved patch-clamp techniques for high-resolution current recording from cells and cell-free membrane patches. *Pflügers Arch.* 391, 85–100.

Helmchen, F., Fee, M.S., Tank, D.W., and Denk, W. (2001). A miniature head-mounted two-photon microscope: high-resolution brain imaging in freely moving animals. *Neuron* 31, 903–912.

Horikawa, K., and Armstrong, W.E. (1988). A versatile means of intracellular labeling: injection of biocytin and its detection with avidin conjugates. *J. Neurosci. Methods* 25, 1–11.

Manns, I.D., Sakmann, B., and Brecht, M. (2004). Sub- and supra-threshold receptive field properties of pyramidal neurones in layers 5A and 5B of rat somatosensory barrel cortex. *J. Physiol.* 556, 601–622.

Margrie, T.W., Brecht, M., and Sakmann, B. (2002). In vivo, low-resistance, whole-cell recordings from neurons in the anaesthetized and awake mammalian brain. *Pflügers Arch.* 444, 491–498.

Markram, H., Lübke, J., Frotscher, M., and Sakmann, B. (1997). Regulation of synaptic efficacy by coincidence of postsynaptic APs and EPSPs. *Science* 275, 213–215.

Martin, S.J., Grimwood, P.D., and Morris, R.G. (2000). Synaptic plasticity and memory: an evaluation of the hypothesis. *Annu. Rev. Neurosci.* 23, 649–711.

Matsumura, M., Chen, D., Sawaguchi, T., Kubota, K., and Fetz, E.E. (1996). Synaptic interactions between primate precentral cortex neurons revealed by spike-triggered averaging of intracellular membrane potentials in vivo. *J. Neurosci.* 16, 7757–7767.

Moore, C.I., and Nelson, S.B. (1998). Spatio-temporal subthreshold receptive fields in the vibrissa representation of rat primary somatosensory cortex. *J. Neurophysiol.* 80, 2882–2892.

Muller, R. (1996). A quarter of a century of place cells. *Neuron* 17, 813–822.

O'Keefe, J., and Dostrovsky, J. (1971). The hippocampus as a spatial map. Preliminary evidence from unit activity in the freely-moving rat. *Brain Res.* 34, 171–175.

Olshausen, B.A., and Field, D.J. (2004). Sparse coding of sensory inputs. *Curr. Opin. Neurobiol.* 14, 481–487.

Paxinos, G., and Watson, C. (1998). *The Rat Brain in Stereotaxic Coordinates*, Fourth Edition (New York: Academic Press).

Pei, X., Volgushev, M., Vidyasagar, T.R., and Creutzfeldt, O.D. (1991). Whole cell recording and conductance measurements in cat visual cortex in-vivo. *Neuroreport* 2, 485–488.

Steriade, M., Timofeev, I., and Grenier, F. (2001). Natural waking and sleep states: a view from inside neocortical neurons. *J. Neurophysiol.* 85, 1969–1985.

Swadlow, H.A., Beloozerova, I.N., and Sirota, M.G. (1998). Sharp, local synchrony among putative feed-forward inhibitory interneurons of rabbit somatosensory cortex. *J. Neurophysiol.* 79, 567–582.

Taube, J.S., Muller, R.U., and Ranck, J.B., Jr. (1990). Head-direction cells recorded from the postsubiculum in freely moving rats. I. Description and quantitative analysis. *J. Neurosci.* 10, 420–435.

Vanderwolf, C.H. (1969). Hippocampal electrical activity and voluntary movement in the rat. *Electroencephalogr. Clin. Neurophysiol.* 26, 407–418.

Yokota, T., Reeves, A.G., and MacLean, P.D. (1970). Differential effects of septal and olfactory volleys on intracellular responses of hippocampal neurons in awake, sitting monkeys. *J. Neurophysiol.* 33, 96–107.

Zhu, J.J., and Connors, B.W. (1999). Intrinsic firing patterns and whisker-evoked synaptic responses of neurons in the rat barrel cortex. *J. Neurophysiol.* 81, 1171–1183.